PSN J14021678+5426205 IN THE GALAXY M 101 AS A MERGER EVENT IN A MASSIVE BINARY SYSTEM

V. P. Goranskij,[1,*] E. A. Barsukova,[2] O. I. Spiridonova,[2]
A. F. Valeev,[2,3] T. A. Fatkhullin,[2] A. S. Moskvitin,[2] O. V. Vozyakova,[1]
D. V. Cheryasov,[1] B. S. Safonov,[1] A. V. Zharova,[1] and T. Hancock[4]

[1]*Sternberg Astronomical Institute, Lomonosov Moscow State University, Universitetskiy pr., 13, Moscow, 119899 Russia*

[2]*Special Astrophysical Observatory of the Russian Academy of Sciences, Nizhniy Arkhyz, Karachai-Cherkessia, 369167 Russia*

[3]*Kazan Federal University, Kremlyovskaya str., 18, Kazan, 420008 Russia*

[4]*Downunder Observatory, Fremont, Michigan, USA*[**]

The observations of the red nova were performed with the Russian 6-m telescope equipped with the SCORPIO focal reducer and with other telescopes of SAO RAS and SAI MSU. We present also the results of investigation of a nova precursor which are based on the Digital Sky Survey and on amateur images available in the Internet. Between April 1993 and July 2014, the brightness of the precursor gradually increased by 2.2 mag V. At the peak of its first outburst in mid-November 2014, the star attained the absolute visual magnitude of -12.75 but was discovered later, in the recurring outburst at -11.65. The outburst amplitude was minimum among red novae, 5.6 mag V only. The spectra showed the Hα emission observed against the backgroung of the continuum of a cool supergiant with the gradually decreasing surface temperature. Such a development is characteristic of red novae, although the studied object showed extreme parameters: the maximum luminosity, the maximum duration of the outburst, the minimum amplitude of the outburst, and the unusual shape of the light curve. This fact was interpreted as a merger of components in the massive system of OB stars which was accompanied by the formation of a common envelope and by the following expansion of this envelope with minimum energy losses.

1. INTRODUCTION

Luminous red novae are representatives of the sparsely populated class of exploding variables which is known since 1988 when such a star exploded in the M 31 galaxy (Red Variable, McD 88 No.1, M31 V1006/7 [1, 2]). Among the galactic red novae, V4332 Sgr, V838 Mon, and V1309 Sco are the most thoroughly studied. According to the archive data, the galactic novae CK Vul (N Vul 1670 [3, 4]), V1148 Sgr (N Sgr 1943 [5]), and OGLE-2002-BLG-360 [6]

* Electronic address: goray@sai.msu.ru
** http://www.downunderobservatory.com

are supposed to belong to this class. The most precise phenomenological definition for the stars of this type is given in [7]: Stars Erupting into Cool Supergiants (SECS). Such "cool explosions" were not predicted theoretically. In the maximum brightness, the absolute magnitudes of red novae exceed those of classical novae and amount up to $M_V = -12^m$ and $-12\overset{m}{.}3$ R (OT 2006-1 in the galaxy M 85 [8, 9] and PTF10fqs in the galaxy M 99 [10]), falling into the interval between the magnitudes of novae and supernovae ($-8^m > M_V > -17^m$ [11]). Red novae, together with other optical transients attaining this range, are called supernovae (SN) impostors, or Intermediate Luminosity Red Transients (ILRT). The remnants of some red novae contain dust and cool rarified gas radiating in atomic and molecular lines.

When explaining the physical nature of outbursts of red novae, the majority of researchers adhere to the hypothesis on the merging of components in a binary or multiple system [12, 13] and call them "mergers". Archive observations of V1309 Sco based on the OGLE data confirmed this hypothesis [14]. Six years before the outburst, this star was a W UMa type contact system with an orbital period of 1.44 day. In this system, merging of components had been monitored directly. It is supposed in [15] that the phenomenon of the red nova arises due to energy splash in the nucleus of the star, after which its envelope enters in the mode of expansion close to adiabatic one (with minimum energy loss), and at that the outburst of the star appears with a time delay of a year or several years. The hypothesis on a "slow shock" which forces the stellar photosphere expand was suggested in [16] in order to explain the phenomenon of the red nova V4332 Sgr. The cause of the slow shock may be both a merger of stellar nuclei in a binary system and an instability of a nucleus of a single star. V838 Mon may be an example of a red nova which is not a merger of components [17]. It is known as a widely detached system containing a type B3 V component [18] which has not take a part in the explosion of 2002 but has been engulfed later by the explosion remnant.

As it follows from the history of research, the most valuable information on the red nova phenomenon can be obtained based on the archive observations and for the stars, the accurate distances of which are possible to determine. Such objects can be those which are situated in the nearby galaxies, although, one needs large telescopes to observe them, as a rule.

In the first half of 2015, two red novae have been discovered in the nearby galaxies, MASTER J004207.99+405501.1 in M 31 (M31N 2015-01a) [19–21] and PSN J14021678 +5426205 (Luminous Red Nova, LRN) in M 101 [22–26]. M31N 2015-01a is similar to V1006/7 in M 31 in maximum brightness $V = 15\overset{m}{.}4$ and in the absolute magnitude $M_V = -9^m$, although, its outburst duration is twice shorter than that of V1006/7. LRN in M 101 reached the absolute

magnitude at the maximum $M_V = -12\overset{m}{.}75$, and possesses unusual properties which have not been observed earlier in other red novae. It is a SN impostor in its absolute magnitude at the brightness maximum. Earlier, four actual SNe of I and II types were observed in M 101: 1909A, 1951H, 1970G, and 2011fe. The present paper is dedicated to the investigation of LRN in M 101.

The red nova in M 101 was discovered by Ciprian Dumitru Vîntdevară [1] on the Bârlad Astronomical Observatory in Romania on February 10, 2015.

We have measured the star brightness in the CCD-image, in which it was discovered, $V = 17\overset{m}{.}50$. According to [23], the star was brighter in the R filter on November 10, 2014, its brightness was $16\overset{m}{.}36$. However, the observations [22] on January 19, 2015 showed the star in a considerably weaker brightness, $R = 18\overset{m}{.}23$ and $V = 18\overset{m}{.}80$. These observations confirmed that the brighter outburst of the star took place in November 2014, and later, the star brightness notably weakened. The star was discovered in the second outburst, the brightness maximum of this outburst was in February 2015.

2. ARCHIVE STUDY OF THE NOVA PRECURSOR

The earliest published observations of the precursor of the LRN outburst in M 101 refer to March 2003 in the SDSS; the magnitudes in the *ugriz* system relative to Vega in these filters are 21.1 ±0.3, 21.6 ±0.3, 21.0 ±0.3, 20.6 ±0.3, and 21.9 ±0.9 respectively [25]. Using the interpolation method, one can determine the values $V = 21\overset{m}{.}2$ and color indices $B - V = 0\overset{m}{.}4$, $V - R_C = 0\overset{m}{.}3$ in the Johnson–Cousins system. From the middle of 2012 to the middle of 2014, the brightness of the star, the precursor of the nova, gradually increased from $20\overset{m}{.}97$ up to $19\overset{m}{.}78$ in the V band, and from $20\overset{m}{.}69$ up to $19\overset{m}{.}59$ in the R band. These observations were found in the archive of the Large Binocular Telescope (LBT) [22].

Reviewing the archives of the Digital Sky Survey, we found out only one weak image of the star in the photo from the Palomar sky survey POSS-II taken with the 48-inch Schmidt telescope on April 15, 1993 using the Kodak IIIaJ emulsion. The maximum sensibility of this emulsion is between the B and V bands. At the time, the star brightness was 22.0 ±0.3 V, from our measurements. To perform the photometric measurements, we created a local standard using several stars in the vicinity of LRN in M 101 with reference to the standard near the blazar S4 0954+65 [27], and then we extended it to the weak magnitudes. Table 1 shows the equatorial coordinates J2000.0 of the standard stars in degrees, by which we can identify the stars in the SDSS Skyserver [2]. The stellar image of the LRN precursor in

[1] http://www.rochesterastronomy.org/snimages/

[2] http://skyserver.sdss.org/dr12/en/tools/chart/navi.aspx

M 101 is present in many amateur color photos of this galaxy in the Internet. The blue color of the star is clearly seen in the photos dated 2011–2013 on Flickr.com, so they obviously contain color information. Terry Hancock performed his observations with the 250-mm astrograph Astro-Tech Richey-Cretien and the monochrome camera QHY9M (with the Kodak chip KAF 8300) and the RGB-filters. The images were collected for 24 hours during five nights from July 14 to 27, 2012 (JD $\approx$ 2456009). We measured the original frames in the FITS format in each filter with reference to the standard in the BVR_C system and obtained the following values and accuracy estimates:

$$B = 21.34^{-0.19}_{+0.22}; \quad V = 21.06^{-0.15}_{+0.16};$$

$$R_C = 20.63^{-0.20}_{+0.25}.$$

Color images we converted them into BITMAP format, and and the separate RGB components were measured relative a R_C, V and B standard, correspondingly. The accuracy of measurements of the color images was within the limits of $0\overset{\mathrm{m}}{.}2$ – $0\overset{\mathrm{m}}{.}3$. We also measured the star in the images by K. Itagaki, the references to which were given in the CBAT. The observations by Itagaki confirm the first and brightest outburst of the star in November 2014 and its further weakening by $2\overset{\mathrm{m}}{.}5$ prior to the second outburst.

Table 2 shows the results of our measurements with the use of the Digital Sky Survey (DSS), the CBAT, and the amateur images in the period from 1993 to 2015, before the discovery, and the published data referring to this time period. The light curves in the BVR_C filters prior to and during the outburst are presented in Fig. 1. Figure 2 shows the color-index curves $B - V$ and $V - R_C$. The total light and color-index curves may be studied in detail in the Internet with a Java-compatible browser [3]. The measurement of brightness and color indices from the amateur images are in a good agreement with the SDSS and LBT observations. These measurements showed that the star brightness prior to the outburst was gradually increasing from a level of $22\overset{\mathrm{m}}{.}0$ V, detected in 1993 in the DSS, up to $19\overset{\mathrm{m}}{.}78$ V, stated with the LBT in summer 2014. The measurements did not make it possible to determine if there was a faster brightness variability at the time of this gradual increase of brightness. Deviations of some measurements from the central trend do not exceed 3σ, as a rule. As is known, the orbital variability was observed in the V1309 Sco red nova system at the time of the brightness increase prior to the outburst. In the case of the LRN in M 101, there was unique information showing that the brightness increased prior to the outburst preserving the stellar surface temperature permanent. The color indices stayed almost constant with $< B - V > \approx 0\overset{\mathrm{m}}{.}2$ and $< V - R_C > \approx 0\overset{\mathrm{m}}{.}2$. At a time, the star moved upward along the main sequence of hot massive supergiants in the Color–Magnitude di-

[3] http://jet.sao.ru/~goray/psn1402.htm

agram $V - (B - V)$ (see Fig. 3). The diagram for normal stars in this figure is plotted based on the photometry from [28] taken with the Hubble Space Telescope. The data are chosen for the area 9492_12 which is located closest to the site of outburst of the LRN in M 101. The red nova is located outside, in $36''$ from its eastern border. The earliest color measurements in 2012 show an evident deviation of the star toward the red side of the OB supergiant branch main sequence; this can indicate the end of the main sequence stage and the start of evolving into red giants of the brighter and more massive component of the system. The position of the star in the diagram in 2012 was close to the position of the well-known massive eclipsing system of high luminosity Hα19 in the galaxy M 33 denoted with the circle in Fig. 3. The orbital period of Hα19 is equal to $33\overset{\mathrm{d}}{.}108$, the absolute magnitude is $\mathrm{M}_V = -7\overset{\mathrm{m}}{.}6$. Mass estimations of the Hα19 system components are 40–50 $\mathrm{M}_\odot$ [29]. This is a semidetached system with so high mass transfer rate that on the surface of its hot component, there is a bright region associated with gas circulation in the envelope of this component forced by the accretion flow from its companion, and with the carrying out the hot material to the surface from the depth of the envelope. The region's light can be seen in the light curve. The earliest observations of the LRN in M 101 in 1993 detected the star at $\mathrm{M}_V = -7\overset{\mathrm{m}}{.}1$. It is weaker than H$\alpha$19 only by $0\overset{\mathrm{m}}{.}5$. Probably, the precursor of the LRN in M 101 was a similar massive system with the mass a bit smaller than that of the Hα19 components.

3. RECENT PHOTOMETRY

The photometric observations of the LRN in M 101 in the second outburst were carried out with several telescopes of SAO RAS and SAI MSU in the BVR_C system from February 15 to July 8, 2015. Table 3 shows the results of brightness measurements, the data on telescopes and instruments used are given in the last column. For the measurements, we used comparison stars from Table 1. The measurement accuracy at a level of $16–18^m$ at the average was $0\overset{\mathrm{m}}{.}01$, at a level of $19–20^m$—$0\overset{\mathrm{m}}{.}02$–$0\overset{\mathrm{m}}{.}04$, weaker 21^m could be up to $0\overset{\mathrm{m}}{.}1$.

According to the observations of the LRN in M 101, in the first outburst the star attained $16\overset{\mathrm{m}}{.}4$ in the V filter in the moment JD 2456975.3 and $16\overset{\mathrm{m}}{.}36$ in the R_C filter in the moment JD 2456971. This corresponds to the absolute magnitudes $\mathrm{M}_V \approx -12\overset{\mathrm{m}}{.}75$ and $\mathrm{M}_R \approx -12\overset{\mathrm{m}}{.}80$. It is visible in the light curve (Fig. 1) that the star brightness in the V filter at the maximum of the first outburst was higher by at least $1\overset{\mathrm{m}}{.}1$ than at the maximum of the second outburst. The same difference between the values in the outbursts turned out to be considerably smaller in the R_C filter, $0\overset{\mathrm{m}}{.}4$. From the observations in the first maximum, we cannot estimate the stellar temperature in the luminosity peak, as the response curves of the amateur instruments are

not known exactly; it is obvious, however, that the star was hotter in the peak of the first outburst than in the peak of the second one. At the maximum of the second outburst, the color indices of the star considerably increased compared to those before the outburst at the end of the gradual brightness increase in summer 2014. $B - V$ increased from $0\overset{m}{.}2$ to $1\overset{m}{.}3$, and $V - R_C$—from $0\overset{m}{.}2$ to $0\overset{m}{.}9$ (Fig. 2) and corresponds to the spectral class K2 I–K3 I. In the R_C band, the star was observed more frequently than in other bands, and the moment of the second maximum could be estimated surely as JD 2457069. At the time, the color indices already were the following: $B - V = 1\overset{m}{.}36 \pm 0.03$ and $V - R_C = 0\overset{m}{.}87 \pm 0.01$. The decline of brightness in the R_C filter in the period JD 2457080—2457132 continued with an average velocity of $0\overset{m}{.}041$/day, and then stopped for 30 days at the brightness level of $18\overset{m}{.}95$ R_C. Later, the brightness decline proceeded with the twice lower velocity. In the V and B filters, the brightness decline rates were notably higher, $0\overset{m}{.}044$ and $0\overset{m}{.}055$ per day respectively; stopping or slowing down of the brightness decline took place in these filters too, although, this was not monitored so thoroughly as in the R_C filter. In the Color–Magnitude diagram, the position of the star at the moment of the brightness stoppage is marked with an asterisk (5). At the time, the star was a red supergiant with the luminosity exceeding the one of the extreme red supergiant from the area 9492_12 in the M 101 galaxy [28] by $1\overset{m}{.}7$. After the brightness decline stopped, the star went on evolving toward red supergiants and in June 2015 attained the position marked with an asterisk (6) in Fig. 3. Multicolor photometry conducted on June 11 yields the following values: $V = 20\overset{m}{.}55$; $B - V = 1\overset{m}{.}83$; $V - R_C = 1\overset{m}{.}27$.

According to the multicolor photometry results, the star can be reliably classified as a luminous red nova, although, its light curve has a specific feature distinguishing it from other red novae: the second outburst. Secondary outbursts were also observed in the red nova V838 Mon, however, with a considerably smaller amplitude. Those outbursts were explained by shock waves coming out to the surface, which were caused by pulsations [30, 31], or swallowing of three massive planets by the expanding red giant [32].

4. SPECTROSCOPY

Spectroscopic observations of medium resolution were carried out at SAO RAS with the 6-m BTA telescope and the SCORPIO focal reducer [33] on February 24 and June 11, 2015. Table 4 contains the main data on the obtained spectra: date, Julian day, full exposure in seconds, spectral range, spectral resolution, grism, heliocentric correction, and the signal-to-noise ratio in continuum in the middle of the spectral range. The reduction of the spectra was made in OS Linux using the ESO MIDAS environment and the LONG context (for the long-slit spectra). The spectra obtained on June 11, 2015 were dis-

torted by fringes at wavelengths $\lambda > 6800$ Å. To compensate the fringes, we obtained the spectra with the shift of the star along the slit. As a result of subtracting the shifted spectra, the sky background was removed together with the fringes. As the signal-to-noise ratio in the total spectrum was too small, we smoothed the spectrum using the moving average method with an averaging interval of 14 Å, which was equal to the actual spectral resolution. To convert the spectra into energy units, we used the spectrophotometric standards HZ 44 and GRW+70°5824 from [34] and simultaneous photometric observations. In digitized form, the spectra are available in the Internet[4]. The moments of the spectral observations are distinguished in the R_C-band light curve (Fig. 4), spectra were taken near the maximum of the second outburst and at the brightness decline which followed after its stoppage.

The total spectrum obtained on February 24, 2015 is shown in Fig. 5, where the strongest lines are marked. Figure 6 shows the fragments of this spectrum with identification of weaker lines. The continuum of a cool star predominates in the spectrum. From the collection of spectra [35], the star HD 1069 (K2 I) best approximates the energy distribution of the LRN. The Hα line is asymmetric, fully in emission with the intensity maximum at a velocity of 300 km/s, the equivalent width EW = −28 Å, the profile halfwidth FWHM = 535 km/s (instrumental-profile corrected). Note that the heliocentric velocity of the galaxy M 101 equals 241 ±2 km/s (from the NED database). The emission expands toward the red side of the spectrum by 20 Å, and toward the blue region by 10 Å, the full width of the line equals FWZI = 1370 km/s. The Ba II λ 6496 Å line, the Ba II λ 6136, 6142 Å blend, and the Na I D_2D_1 λ 5890, 5896 Å blend have emission components in their P Cyg type profiles, the maximum of emission intensity in these profiles is located at 330 km/s. The absorption components of these lines at the intensity minimum have a velocity of −260 km/s and expand blueward to −620 km/s. The lines H_β, Ba II λ4709, 4957, 5874 Å, Mg I λ 5167, 5173 Å, and numerous Fe I, Ti I, Cr I lines are observed in absorption. Radial velocities of these lines are similar to the velocities in absorption components of the P Cyg type profiles of the strong lines. The set of absorption lines of chemical elements duplicates in detail the set of lines for the red nova V838 Mon in the January 2002 in outburst, when its spectrum was classified as K0 I [36]. The significant difference with the LRN spectrum was the absence of the Li I λ 6708 Å line, which was very strong in the V838 Mon spectrum and had a P Cyg profile.

From the observations carried out in February, the velocity of the envelope expansion of the LRN in M 101 at the peak of the second outburst was 500 − 540 km/s. As a comparison, the velocity of the envelope expansion of V838 Mon at the outburst peak was 150 km/s, 3.5 times lower.

[4] http://jet.sao.ru/~bars/spectra/psn1402/

Cross-correlation of the LRN/M101 normalized spectrum of February 24, 2015 with the normalized spectra of the supergiants from [35] determines the LRN spectrum in a wider range as K0 I - K5 I (from the spectral lines). The strength of absorption lines in the LRN/M101 spectrum 4 – 6 times exceeds the strength of the lines of normal stars. That is why, there are depressions in the LRN spectrum in the ranges of λ 5000 – 5500 Å and 6100 – 6400 Å visible due to line blocking of the continuum.

Figure 7 shows the red nova spectrum obtained on June 11, 2015. This spectrum has three times lower resolution and, therefore, the narrow absorption lines are seen not so clearly as in the February spectrum. Energy distribution in the spectrum became redder and can be best approximated with the distribution of the star HD 13136 (M2 Ib), although, there are no more late spectral type stars among the stars of luminosity I type for comparison in [35]. From the color index $B - V = 1\overset{\mathrm{m}}{.}83 \pm 0\overset{\mathrm{m}}{.}10$, this is a star of the spectral type M1 I – M4 I. The H_α emission with an equivalent width of EW = −107 Å predominates, it is more symmetric than in the February spectrum. Its instrumental-profile corrected half-width is equal to FWHM = 900 km/s. The heliocentric radial velocity is ≈150 km/s. In this line, one can see weak emission wings which determine the full width FWZI = 189 Å (8600 km/s). These wings probably develop due to Thompson scattering. Probably, a weak emission presents in H_β and Na I D_2D_1.

The TiO bands can be noticed in the absorption spectrum, the strongest of which have heads at wavelengths of λ 4955, 5450, 5498, 5597, 6159, 6659, 6715, 6817, 7054, 7090, 7126, and the strongest one—at λ 7589 Å. Atomic absorptions can be hardly seen due to the low resolution, only the triplet Mg I λ 5167 – 5183 Å and some Fe I blends have been identified.

Spectral observations, as well as the photometry, show the energy distribution shift towards the red region. These are low-excitation spectra in which the atomic lines predominate and then the molecular lines appear at the brightness decline. Such development is characteristic of red novae.

5. DISCUSSION OF RESULTS

The LRN in M 101 turned out to be a massive young star, the outburst of which took place in the spiral arm of the M 101 galaxy in the region of an association of hot OB-supergiants. It is not associated with nebulae. Red novae belong to different types of galaxy populations and show the variations in amplitudes, in outburst durations, and in the shapes of light curves. PTF10fqs emerged in the spiral arm of the M 99 galaxy and was associated with the OB-supergiant association as well as the LRN in M 101 [10]. The other red nova PTF10acbp has exploded in the outskirts of the spiral galaxy UGC 11973 [37] and obviously belongs to the

young population of the disk. The red nova OT 2006-1 appeared in the outskirts of the M 85 galaxy, classified as S0, and evidently was not associated either with the H II region or with any other star formation region [38]. The red nova V838 Mon is associated with the population type I of the Galaxy and with the young cluster of B-stars [**?**]. V1006/7 in the M 31 galaxy, the Galactic red novae V4332 Sgr and V1309 Sco are the objects of a galactic bulges or a thick disks. In the V4332 Sgr system, there is an evolved star, a red giant, the radiation of which is detected in energy distribution of the outburst precursor and also in the spectrum after the outburst [15]. The last three objects are obviously old stellar systems which got though the long-term evolution process.

The duration of red novae outbursts varies in the range of 58 days (in the V filter, M31N 2015-01a) to 135 days (in the R filter, PTF10fqs/M 99), if the visibility time above a level of 3^m lower than the maximum brightness is considered. Red nova outbursts have similar light curves: the slow brightness weakening immediately after the maximum ("flat maximum" or "plateau"), which ends in the steep fall, although, there are some exceptions. In the V838 Mon outburst, several local maxima were observed, they were accompanied by the temperature increase and emerging of the emission lines of ionized elements in the spectrum, which can be associated with the coming out of the shock waves to the expanding envelope surface. The LRN in M 101 exceeds all other red novae in the outburst duration. If we estimate the second outburst duration by this criterion, we obtain 154 days (in the V filter); in case we count from the first outburst in November 2014, which was brighter at the maximum, we obtain more than 153 days. Therefore, the outburst of the LRN in M 101 is the longest. There are some other special features of the light curve of the LRN in M 101 becoming apparent when compared to other red novae. In the second outburst in February 2015, neither flat maximum nor steep fall were observed. Moreover, there was the stoppage of the brightness decline for 30 days. It is interesting that in the V1309 Sco red nova there were two similar stops in the brightness decline (see fragments 9 and 10 in the light curve if Figs. 1 and 2 in [14]). These stops in the brightness decline can also be associated with the weaker shock waves on the surface of the envelope. It should be noted that the shape of the V1309 Sco light curve also differed from those of other red novae in the absence of the flat maximum and the brightness decline after the outburst was gradual and with the following deceleration.

If we take the brightness observed in 1993 (DSS, POSS II) as a reference point for the LRN in M 101, then the outburst amplitude will be equal to $5\overset{\mathrm{m}}{.}6$, which is the lowest amplitude measured for a red nova. Still, in absolute magnitude at the brightness first maximum, $\mathrm{M}_V = -12\overset{\mathrm{m}}{.}75$, it is probably the most luminous red nova. The star OT 2006-1 in the galaxy

M 85 attained the same absolute magnitude but in the red range, $M_R = -12\overset{m}{.}7$ [9] (the authors classified it as SN IIp).

The characteristic feature of the light curve of the LRN in M 101 is the gradual increase of brightness before the outburst, which amounted at least $2\overset{m}{.}2$. As follows from the observations of the red nova V1309 Sco [14], such an increase in brightness takes place when the common envelope is forming before a star merger in a contact system; thus, the development of the LRN in M 101 in 2015 most probably is a "merger"—merging of the system components. In the case of V1309 Sco, the gradual brightening finished a year before the maximum with the abrupt light decay by $1\overset{m}{.}$ In the case of the LRN/M 101, the brightness weakening was not detected between the last observation at the brightness increase stage in July 2014 (LBT, [22]) and the first observation at the outburst peak on November 10, 2014 (PTF, [23]). Such brightness weakening can be expected in case of the common envelope expansion in the mode similar to adiabatic as a result of the energy splash and the pulse inside at the merging of two stars' cores. However, we can see the result of such an expansion in the second outburst as a considerable reddening of the color indices. Under the assumption that the common envelope had already formed by July 2014, using the Stefan-Boltzmann law and the photometric parameters of the star, we estimated that the envelope radius varied by a factor of 8, from 400 $R_\odot$ in July 2014 to 3300 $R_\odot$ in February 2015. In July 2015, the envelope radius grew up to 4700 $R_\odot$. These estimates can be inaccurate because of the complex structure of the outburst debris, however, they prove that the expansion of the envelope, possessing the photosphere, took place in the period between July 2014 and February 2015. The velocities determined from the absorption lines and components in the P Cyg type profiles ($500 - 540$ km/s) do not correspond to such envelope radius variations estimated with the Stefan-Boltzmann method, and 2–3 times exceed these estimates. The similar effect was also observed in V838 Mon.

Taking into consideration that the observed velocities of the envelope expansion of the LRN in M 101, determined from the absorption components and lines, are three times greater than the velocities of the envelope expansion of V838 Mon and V1309 Sco at this stage, the duration of the envelope expansion can be significantly shorter, only several months. As the outburst developed at such great rates, it could be assumed that earlier, when the stars' cores merged and there was the energy pulse from the inside, the shock wave formed, and the first outburst in November 2014 was associated with emerging of this shock wave. It was most probable that when the shock wave emerged, some layer absorbing in lines separated from the envelope and moved at a higher velocity than the photosphere. It is exactly due to this additional layer both in the LRN in M 101 and in V838 Mon, the absorption line spectrum is 4–6 times stronger than the that of

normal stars of the same spectral type.

After emerging of the shock wave, the envelope expanded with the decrease of energy output during December 2014 and January 2015, which resulted in the brightness decrease at least by $2\overset{\mathrm{m}}{.}4$. It is not improbable that the shock wave formation in the LRN in M 101 is associated with the great mass of this system. The second outburst in February 2015 is an arrival of the outburst thermal energy to the surface of the expanding envelope. This scenario can be confirmed or disproved by the model dynamic calculations or archive observations if they are taken in the period between July 2014 and February 2015.

6. CONCLUSIONS

The LRN in M 101 has emerged in the spiral galaxy in the region of the OB-star association and is a massive system, the bright component of which leaves the main sequence of the Color-Magnitude diagram toward the red side. Over 11 years prior to the outburst, the brightness of the system gradually increased by $2\overset{\mathrm{m}}{.}2$. As the brightness increase before the outburst takes place when the components move closer and the common envelope forms, we identify this event with the merger of the components in the massive system.

The star had an unusual light curve with two peaks of luminosity. The star was discovered in the second outburst that followed three months after the first maximum, in which it attained the visual absolute magnitude -12.75. The star envelope expanded prior to the second outburst increasing its radius by a factor of 8. In the second outburst maximum, the star spectrum was classified as ∼K2 I and in three months it evolved with the temperature decrease to ∼M2 I. In the K2 I spectrum, we detected the Hα emission, strong Ba II and Na I lines with the P Cyg profiles, and the extremely strong absorbtion in the metal lines Fe I, Ti I, Cr I, and Mg I. Formation of such a spectrum is obviously associated with the ejection of the absorbing layer at the shock wave arrival in the first outburst. The rates of the absorbing layer expansion are 500–540 km/s. The weak TiO molecular bands can be seen in the M2 I spectrum. The spectral development is characteristic for red novae and leaves no doubt about the classification.

Among the known red novae, the outburst of the LRN in M 101 is record in the duration (a visibility of $>$153 days above the level of 3^m lower than the maximum level), in the absolute visual magnitude at the maximum (–12.75), and in the outburst amplitude ($5\overset{\mathrm{m}}{.}6$ V) which is the smallest of the measured ones.

ACKNOWLEDGMENTS

In the paper, we used the following databases: Sloan Digital Sky Survey, NASA/IPAC Extragalactic Database (NED), Vienna Atomic Line Database (VALD), NIST Atomic Spectra

Database, SuperCOSMOS Sky Survey, and web-hostings for images AstroBin and Flickr. The spectral and photometric observations, their reduction and analysis carried out at SAO RAS were financed with the Grant of the Russian Science Foundation No. 14-50-00043. V.P.G., E.A.B., and A.F.V. are grateful to the Russian Foundation for Basic Research for the financial support with the grant No. 14–02–00759. A.S.M. wishes to thank the President of the Russian Federation for the financial support with the Grant MK-1699.2014.2. The observations at the Russian 6-m BTA telescope are carried out with the financial support of the Ministry of Education and Science of the Russian Federation (agreement No. 14.619.21.0004, project ID RFMEFI61914X0004). In our work, we used the instruments created with the support from the M.V. Lomonosov Moscow State University Development Program.

---

1. \refitem{***article***}
R. M. Rich, J. Mould, A. Picard, et al., Astrophys. J. **341**, L51 (1989).
2. \refitem{***article***}
A. S. Sharov, Astronomy Letters **19**, 83 (1993).
3. \refitem{***article***}
M. Hajduk, P. A. M. van Hoof, A. A. Zijlstra, Monthly Notices Roy. Astronom. Soc. **432**, 167 (2013).
4. \refitem{***article***}
T. Kaminski, K. M. Menten, R. Tylenda, et al., Nature **520**, 322 (2015).
5. \refitem{***article***}
M. W. Mayall, Astronom. J. **54**, 191 (1949).
6. \refitem{***article***}
R. Tylenda, T. Kaminski, A. Udalski, et al., Astronom. and Astrophys. **555**, 16 (2013).
7. \refitem{***book***}
U. Munari, A. Henden, R. M. L. Corradi, T. Zwitter, in *Classical Novae Explosions*, Ed. M. Hernanz, J. Jose, AIP Conf. Proc. **637**, 52 (2002).
8. \refitem{***article***}
S. R. Kulkarni, E. O. Ofek, A. Rau, et al., Nature **447**, 458 (2007).
9. \refitem{***article***}
A. Pastorello, M. Della Valle, S. J. Smartt, et al., Nature **449**, E1 (2007) (arXiv: astro-ph 0710.3763).
10. \refitem{***article***}
M. M. Kasliwal, S. R. Kulkarni, I. Arcavi, et al., Astrophys. J. **730**, 134 (2011).
11. \refitem{***article***}
E. Berger, A. M. Soderberg, R. A. Chevalier, et al., Astrophys. J. **699**, 1850 (2009).
12. \refitem{***article***}
N. Soker, R. Tylenda, Astrophys. J. **582**, L105 (2003).
13. \refitem{***article***}
N. Soker, R. Tylenda, Monthly Notices Roy. Astronom. Soc. **373**, 733 (2006).
14. \refitem{***article***}
R. Tylenda, M. Hajduk, T. Kaminski, et al., Astronom. and Astrophys. **528**, 114 (2011).
15. \refitem{***article***}
E. A. Barsukova, V. P. Goranskij, A. F. Valeev, and A. V. Zharova, Astrophys. Bull. **69**,

67 (2014).

16. \refitem{***article***}
P. Martini, R. M. Wagner, A. Tomaney, et al., Astronom. J. **118**, 1034 (1999).

17. \refitem{***book***}
V. Goranskij, N. Metlova, A. Zharova, et al. *Astroplate Proceedings*, Ed. L. Miskova, S. Vitek (Institute of Chemical Technology, Prague, 2014). P.95 (arXiv: astro-ph 1501.03615).

18. \refitem{***misc***}
R. M. Wagner, G. Schwarz, S. Starrfield, et al., IAU Circ., No. 8202 (2003).

19. \refitem{***misc***}
V. Shumkov, M. Pruzhinskaya, N. Tiurina, E., et al., Astronomer's Telegram No. 6951 (2015).

20. \refitem{***misc***}
S. C. Williams, M. J. Darnley, M. F. Bode, I. A. Steele, Astrophys. J. **805**, L18 (2015).

21. \refitem{***misc***}
A. Kurtenkov, P. Pessev, T. Tomov, et al., Astronom. and Astrophys. **578**, L10 (2015).

22. \refitem{***misc***}
J. Gerke, S. M. Adams, C. S. Kochanek, K. Z. Stanek, Astronomer's Telegram No. 7069 (2015).

23. \refitem{***misc***}
Y. Cao, M. M. Kasliwal, G. Chen, I. Arcavi et PTF collaboration, Astronomer's Telegram No. 7070 (2015).

24. \refitem{***misc***}
J. Vinko, K. Sarneczky, A. Szing, Astronomer's Telegram No. 7079 (2015).

25. \refitem{***misc***}
P. Kelly, S. van Dyk, O. Fox, et al., Astronomer's Telegram No. 7082 (2015).

26. \refitem{***misc***}
V. P. Goranskij, D. V. Cherjasov, B. S. Safonov, et al., Astronomer's Telegram No. 7206 (2015).

27. \refitem{***article***}
C. M. Raiteri, M. Villata, G. Tosti, et al., Astronom. and Astrophys. **352**, 19 (1999).

28. \refitem{***article***}
S. Grammer, R. M. Humphreys, Astrophys. J. **146**, 114 (2013).

29. \refitem{***book***}
V. P. Goranskij, E. A. Barsukova, in *Active OB Stars: Structure, Evolution, Mass Loss, and Critical Limits*, Ed. C. Neiner, G. Wade, G. Meynet, & G. Peters (IAU Symp. 272, Paris, 2010), p. 610 (2011).

30. \refitem{***book***}
E. A. Barsukova, N. V. Borisov, V. P. Goranskij, et al., in *Classical Novae Explosions*, Ed. M. Hernanz, J. Jose, AIP Conf. Proc. **637**, 303 (2002).

31. \refitem{***book***}
V. P. Goranskij, N. V. Metlova, S. Yu. Shugarov, et al., in *The Nature of V838 Mon and its light echo*, Ed. R. L. M. Corradi & U. Munari, ASP Conf. Series **363**, 214 (2007).

32. \refitem{***article***}
A. Retter, A. Marom, Monthly Notices Roy. Astronom. Soc. **345**, L25 (2003).

33. \refitem{***article***}
V. L. Afanasiev, A. V. Moiseev, Astron. Lett. **31**, 194 (2005).

34. \refitem{***article***}
J. B. Oke, Astronom. J. **99**, 1621 (1990).

35. \refitem{***article***}
G. H. Jacoby, D. A. Hunter, C. A. Christian, Astrophys. J. Suppl. **56**, 257 (1984).

36. \refitem{***article***}

V. P. Goranskij, A. V. Kusakin, N. V. Metlova, et al., Astronomy Letters **28**, 691 (2002).

37. \refitem{***misc***}
M. M. Kasliwal, S. R. Kulkarni, E. O. Ofek, et al., Astronomer's Telregram No. 3094 (2010).

38. \refitem{***article***}
E. O. Ofek, S. R. Kulkarni, A. Rau, et al., Astrophys. J. **674**, 447 (2008).

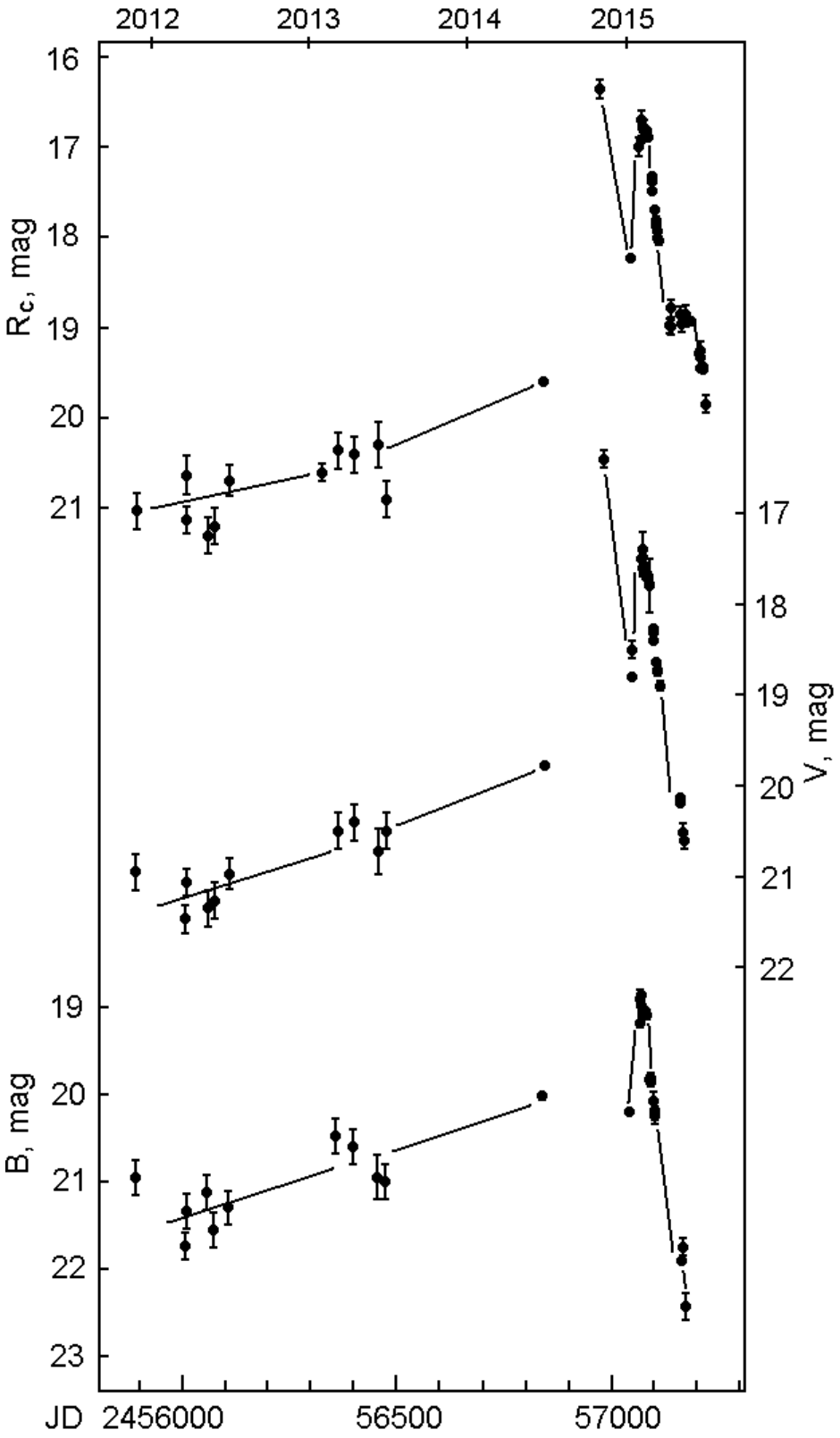

Figure 1. Light curves of the LRN in M 101 in 2012–2015 in the B, V, R bands (from bottom to top).

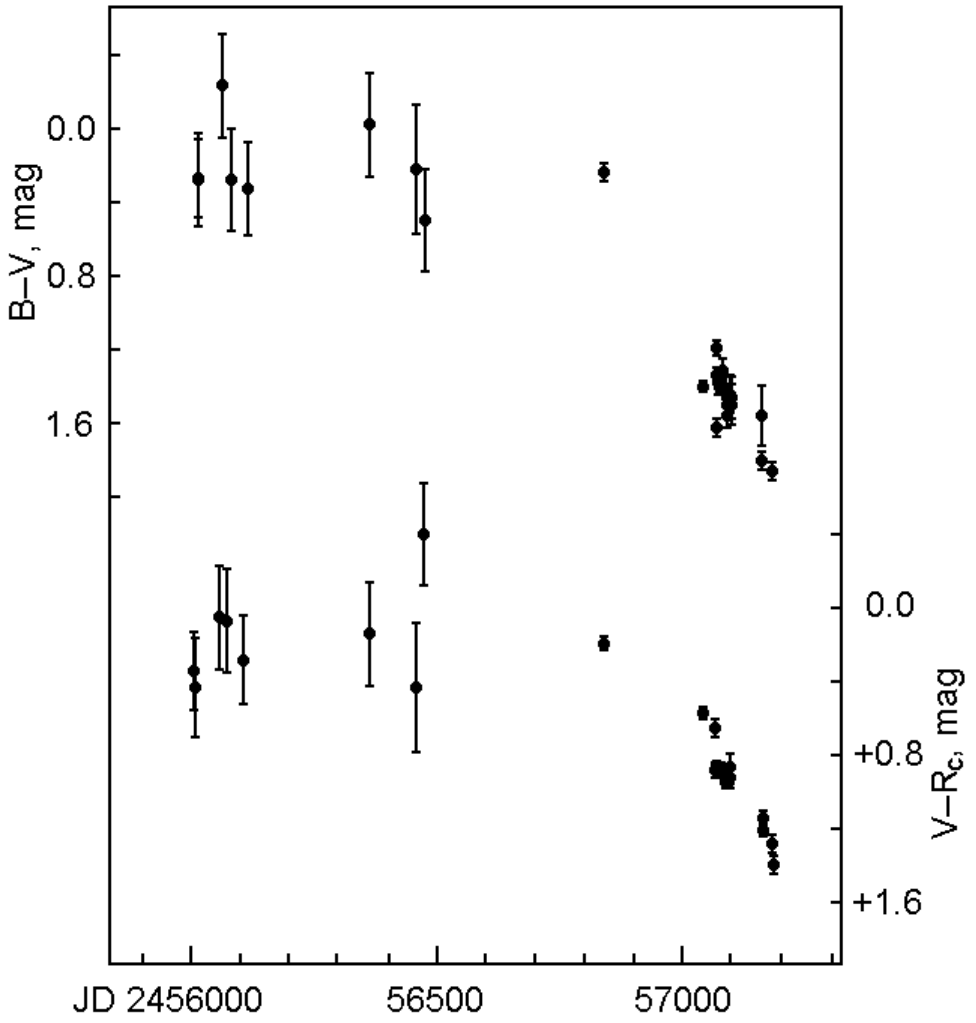

Figure 2. Color index curves $B-V$ (top) and $V-R_C$ (bottom) constructed for the LRN in M 101 from the observations in 2012–2015

Table 1. BVR-magnitudes of the comparison stars in the vicinity of the LRN in M 101

Star No.	R.A. deg.	Decl. deg.	B mag.	V mag.	R_C mag.
1	210.57966	54.44921	16.145	15.056	14.325
2	210.57058	54.45812	18.006	16.879	16.024
3	210.55809	54.44282	20.23	19.62	19.14
4	210.65176	54.44635	17.092	16.120	15.501
5	210.63700	54.44778	17.612	16.497	15.730

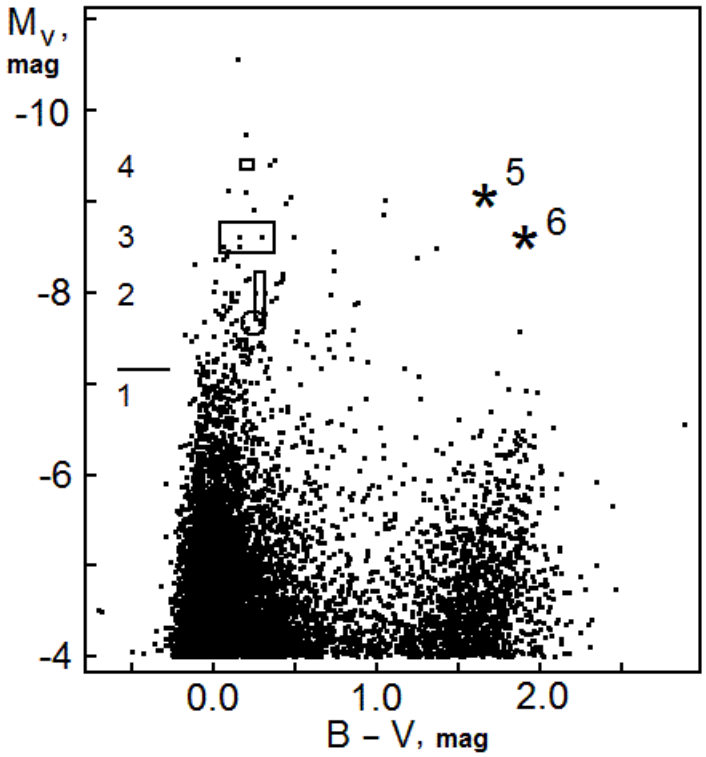

Figure 3. Shift of the LRN/M 101 precursor in the Color – Absolute magnitude diagram before the outburst in 2014. 1 – the brightness level in 1993 according to the data from POSS-II. The rectangles: 2 – the position in the diagram in 2012; 3 – this one in 2013, and 4 – the position in the middle of 2014 [22]. Asterisks: 5–the position of the star at the brightness decline stop in May 2015, and 6–in the middle of June 2015. The circle – the position of the semi-detached massive system Hα19 from the galaxy M 33 with the high mass transfer rate in the phase of the components merging. The diagram is constructed for the area 9492_12 in the galaxy M 101, which is the closest to the LRN in M 101. This is the photometry [28] based on the archives of the Hubble Space Telescope (the LRN in M 101 does not belong to this area but is located close to its boundary).

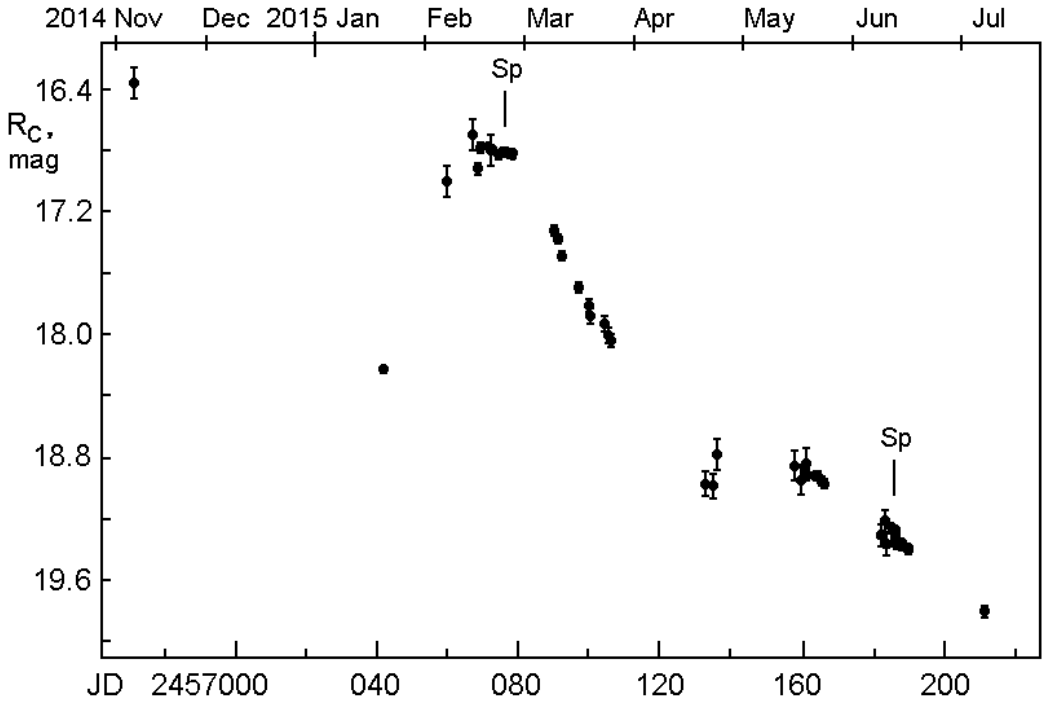

Figure 4. Light curve of the LRN in M 101 in the R_C band plotted for the second outburst. Signs "Sp" denote the times of spectral observations with the BTA/SCORPIO.

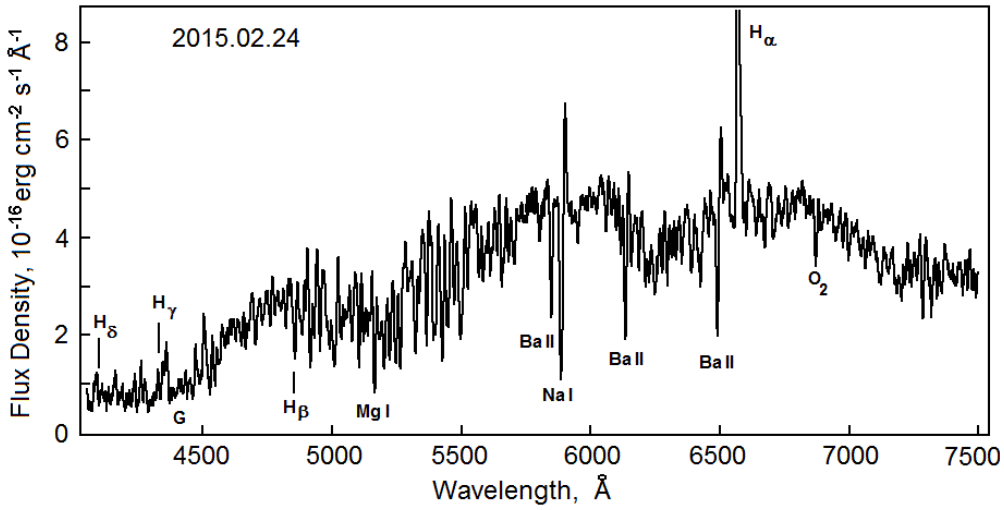

Figure 5. Spectrum of the LRN in M 101 obtained with the BTA telescope and the SCORPIO camera on February 24, 2015 near the maximum of the second outburst.

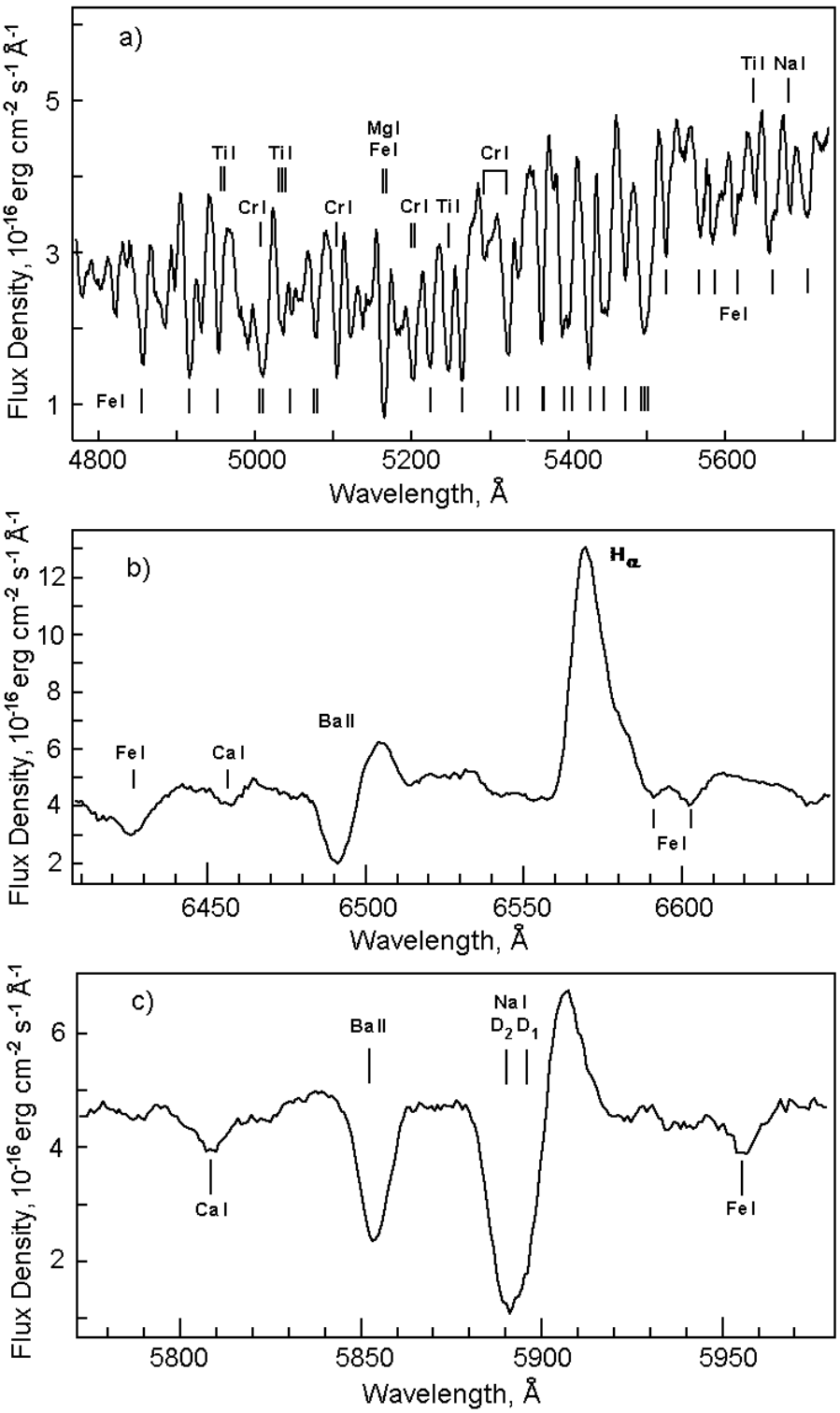

Figure 6. Fragments of the LRN in M 101 spectrum obtained on February 24 and identification of the spectral lines. a – the depression region λ5000 – 5500 Å associated with atomic line absorption. b – H_α and Ba II 6496 Å line profiles. c – Na I D_2D_1 and Ba II 5854 Å line profiles.

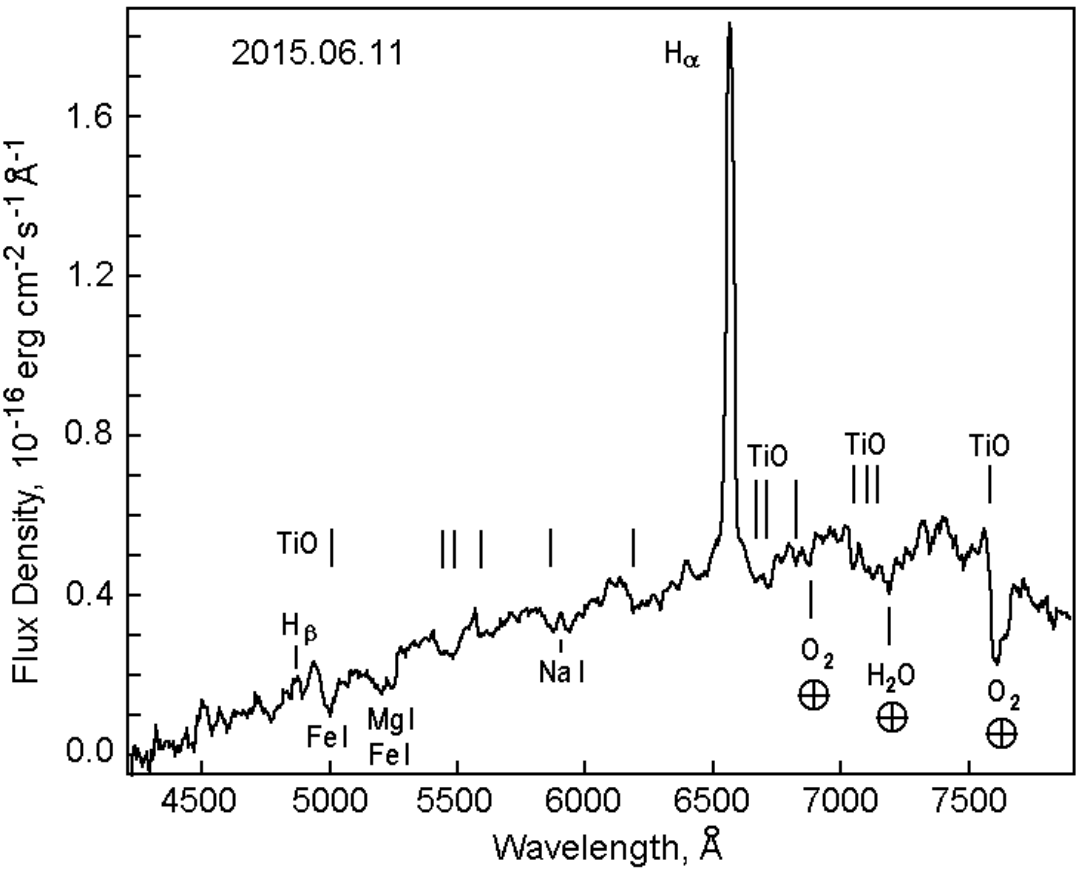

Figure 7. Spectrum of the LRN in M 101 taken with the BTA telescope and the SCORPIO camera on June 11, 2015. The original spectrum with a small S/N ratio is averaged with the interval 14 Å corresponding to the spectral resolution. Sign $\oplus$ denotes the molecular bands of the telluric origin.

Table 2. Pre-discovery observations of the LRN/M101

Date	JD 24...	B	V	R	Source
1993.04.15	49093	-	22.0	-	POSS II, Kodak IIIaJ
2003.03.07-10	52707	21.6	21.2	20.90	SDSS, ATel 7082[1])
2011.11.25	55891	20.95	20.95	21.03	R. Pecce, Flickr.com
2012.03.20	56007	21.74	21.47	21.13	D. Hartmann, Astrobin[2])
2012.02.14-27	56009	21.34	21.06	20.63	T. Hankock, RGB images[3])
2012.05.10	56058	21.12	21.35	21.30	O. Bryzgalov, Flickr.com
2012.05.26	56074	21.55	21.27	21.20	O. Bryzgalov, Flickr.com
2012.01-06	56109	21.30	20.97	20.69	ATel 7069, LBT
2013.02.01	56324	-	-	20.60	ATel 7070, PTF
2013.04	56360	20.48	20.50	20.36	Z. Orbanic, Flickr.com[4])
2013.03-05	56398	20.6	20.4	20.40	R. Pfile, Flickr.com
2013.06.11	56455	20.95	20.73	20.30	S. Furlong, Flickr.com
2013.06.29	56473	21.0	20.5	20.9	C. Frenzi, Flickr.com
2014.06-07	56839	20.02	19.78	19.59	ATel 7069, LBT
2014.11.10	56971	-	-	16.36	ATel 7070, PTF
2014.11.13	56975	-	16.40	-	K. Itagaki, CBAT[5])
2015.01.19	57042	20.20	18.80	18.23	ATel 7069, LBT
2015.01.20	57043	-	18.50	-	K. Itagaki, CBAT[5])
2015.02.10	57064.4	-	17.50	-	C. D. Vintdevara, discovery

[1]) SDSS-values in the *ugriz* (Vega) system recounted to the BVR_C system.

[2]) http://www.astrobin.com/users/DetlefHartmann/

[3]) 25-cm Ritchey-Chretien astrograph + the CCD QHY9M Monochrome (Kodak KAF 8300 chip), 24-hour exposure.

[4]) Uploaded on June 30, 2014. The approximate time of imaging, April 2013, can be determined from the brightness of SN 2011fe.

[5]) http://www.cbat.eps.harvard.edu/unconf/followups/J14021678+5426205.html

Table 3. Photometry of the LRN in M 101

JD hel.24...	B	V	R_C	rem.	JD hel.24...	B	V	R_C	rem.
57069.3642	-	17.664	16.776	KG	57105.5199	-	-	18.009	SO
57069.4892	18.862	17.666	16.784	KG	57106.3993	-	18.901	18.041	SO
57071.5603	18.988	17.649	16.771	SO	57133.2957	-	-	18.977	SO
57071.5784	-	17.655	16.776	SO	57135.5288	-	-	18.991	SO
57072.5776	19.034	17.667	16.803	SO	57136.4051	-	-	18.785	SO
57072.5894	-	17.663	16.793	SO	57158.3471	-	-	18.859	SO
57074.5439	19.086	17.708	16.825	KG	57160.3074	-	-	18.952	SO
57075.5213	19.045	17.704	16.815	SO	57161.3043	-	-	18.915	SO
57075.5326	-	17.669	16.808	SO	57162.3288	-	-	18.853	SO
57076.5682	19.082	17.687	16.815	SO	57163.3073	-	-	18.928	SO
57076.5790	-	17.690	16.808	SO	57164.3126	21.87	20.075	18.928	SO
57077.5862	19.066	17.690	16.826	SO	57165.3147	21.70	20.160	18.954	SO
57077.5793	-	17.699	-	SO	57166.3898	-	20.158	18.967	SO
57078.3967	19.088	17.698	16.827	SO	57182.3213	-	-	19.291	SO
57078.4095	-	17.708	16.829	SO	57183.2694	-	-	19.334	CR
57078.4318	19.037	17.691	16.816	6m	57183.3529	-	-	19.233	SO
57081.5474	19.086	17.784	16.901	KG	57184.34	-	20.72	19.267	SO
57081.5639	-	17.796	16.896	KG	57185.29	22.38	20.55	19.278	SO
57090.4413	19.832	18.268	17.325	SO	57185.3360	-	-	19.352	6m
57090.4628	-	18.295	17.322	SO	57185.3373	-	-	19.313	6m
57091.5366	19.814	18.305	17.375	SO	57185.3382	-	-	19.316	6m
57091.5485	-	18.307	17.380	SO	57186.2240	-	-	19.332	CR
57092.5591	19.856	18.399	17.489	SO	57186.3192	-	-	19.330	SO
57097.3654	20.070	18.633	17.696	SO	57187.2308	-	-	19.374	CR
57100.3466	20.190	18.730	17.814	SO	57187.3792	-	-	19.365	SO
57100.3919	20.241	18.742	17.881	SO	57211.4180	-	-	19.820	SO
57104.5638	-	-	17.931	SO					

Remarks:

6m – BTA and SCORPIO spectral camera with the BVR_CI_C filters [33];

KG – 2.5-m telescope of the SAI MSU Caucasus Mountain Observatory with the CCD-cameras Proline KAF 39000 and NBI 2k2k with the BVR_CI_C filters;

SO – 1-m Zeiss telescope of the SAO RAS and the $UBVR_CI_C$-photometer with the CCD EEV 42-40 chip;

CR – 0.6-m Zeiss telescope of the SAI MSU Crimean Station and the $UBVR_CR_JI_J$-photometer with the CCD camera Apogee-47p.

Table 4. Spectra of the LRN in M 101 obtained with the BTA/SCORPIO

Date	JD hel.24...	ϵ, A	λ, Å	R, Å	Grism	Δv_r, km/s	S/N
2015.02.24	57078.4531	2400	4052 – 5848	5.0	VPHG1200G	+5.0	180
2015.02.24	57078.5829	2751	5751 – 7498	5.0	VPHG1200R	+4.9	50
2015.06.11	57185.3412	3600	4000 – 7919	14	VPHG500G	–14.9	12